

1
2
3
4
5
6
7
8
9
10
11
12
13
14
15
16
17
18
19
20
21
22
23

The Assumption of Poisson Seismic-Rate Variability in CSEP/RELM Experiments

A.M. Lombardi & W. Marzocchi

Istituto Nazionale di Geofisica e Vulcanologia, Via di Vigna Murata 605, 00143 Rome, Italy.

Revised version, submitted to BSSA

2010

24 **Abstract**

25 Evaluating the performances of earthquake forecasting/prediction models is the main rationale
26 behind some recent international efforts like the Regional Earthquake Likelihood Model (RELM)
27 and the Collaboratory for the Study of Earthquake Predictability (CSEP). Basically, the evaluation
28 process consists of two steps: 1) to run simultaneously all codes to forecast future seismicity in
29 well-defined testing regions; 2) to compare the forecasts through a suite of statistical tests. The tests
30 are based on the likelihood score and they check both the time and space performances. All these
31 tests rely on some basic assumptions that have never been deeply discussed and analyzed. In
32 particular, models are required to specify a rate in space-time-magnitude bins, and it is assumed that
33 these rates are independent and characterized by Poisson uncertainty. In this work we have explored
34 in detail these assumptions and their impact on CSEP testing procedures when applied to a widely
35 used class of models, i.e., the Epidemic-Type Aftershock Sequence (ETAS) models. Our results
36 show that, if an ETAS model is an accurate representation of seismicity, the same "right" model is
37 rejected by the current CSEP testing procedures a number of times significantly higher than
38 expected. We show that this deficiency is due to the fact that the ETAS models produce forecasts
39 with a variability significantly higher than that of a Poisson process, invalidating one of the main
40 assumption that stands behind the CSEP/RELM evaluation process. Certainly, this shortcoming
41 does not negate the paramount importance of the CSEP experiments as a whole, but it does call for
42 a specific revision of the testing procedures to allow a better understanding of the results of such
43 experiments.

44

45

46 **1. Introduction**

47 The success of operational forecast indispensably depends on the use of reliable and skillful models
48 (ICEF, 2009). In a nutshell, a model has to produce forecasts/predictions compatible with the future
49 seismicity, and the forecasts/predictions have to be precise enough to be usable for practical

50 purposes (i.e., they need a good skill). Moreover, if a set of reliable models is available, it is
51 important to know what is the "best" one(s), i.e., the one(s) with the highest skill.

52 The evaluation of these pivotal features characterizing each forecasting/prediction model is the
53 primary goal of the Collaboratory for the Study of Earthquake Predictability (CSEP hereinafter;
54 Jordan 2006; <http://www.cseptesting.org>).

55 CSEP provides a rigorous framework for an empirical evaluation of any forecasting and prediction
56 model. CSEP can be considered the successor of the Regional Earthquake Likelihood Model
57 (RELM) experiment (Schorlemmer and Gerstenberger, 2007). While RELM was focusing on
58 California, CSEP extends this focus to many other regions (New Zealand, Italy, Japan, North- and
59 South-Western Pacific, and the whole World) as well as global testing centers (New Zealand,
60 Europe, Japan). The coordinated international experiment has two main advantages: the evaluation
61 process is supervised by an international scientific committee, not only by the modelers themselves,
62 and the cross-evaluation of a model performances in different regions of the world can facilitate its
63 evaluation in a much shorter period of time (see also Zechar et al., 2009).

64 All CSEP experiments performed in each testing region are truly prospective tests. In other words,
65 each experiment compares forecasts produced by several models under testing with real data
66 observed in the corresponding testing region after the forecasts have been produced. The forecasts
67 are generated in the testing center independent of the modelers. The testing procedure adopted can
68 be summarized in two subsequent steps: 1) to measure the *reliability* of each model; 2) to quantify
69 the relative *skill* among the set of reliable models. In the first step, the forecasts/predictions made by
70 each model are compared to the real seismicity through one or more goodness-of-fit tests. If the
71 seismicity observed is compatible with the output of the model and the model-based variability,
72 then the performance of the models can be contrasted with other models in the second step of the
73 analysis. Specifically, the second step of the analysis compares quantitatively the
74 forecasting/prediction capabilities of the models in order to establish a hierarchy of best performing
75 models.

76 In this paper, we explore the performances of the CSEP/RELM testing procedure for two classes of
 77 forecasting models, Poisson and ETAS, that are largely represented in CSEP/RELM experiments
 78 (for the reliability of the prediction models see, e.g., Marzocchi et al., 2003; Zechar & Jordan, 2008,
 79 and references therein).

80

81 **2. The CSEP/RELM suite of tests**

82 The CSEP/RELM suite of tests is originally composed of three different tests (Schorlemmer et al.,
 83 2007; see also Kagan and Jackson 1994; 1995). The *L*-test (*Data-consistency test*) and *N*-test
 84 (*Number of events test*) are intended to check the goodness-of-fit of the model, while the *R*-test
 85 (*Hypotheses comparison*) compares the forecasting performances of different models.

86 The *L*-test and *R*-test are based on the well-known concept of conditional likelihood that is one of
 87 most used statistical tools to check and compare the performance of one or more models on data.
 88 The formulation of these tests requires the definition of bins that are specified intervals in space,
 89 magnitude and time. Using the same symbols of *Schorlemmer et al. (2007)*, we define:

ω_i number of earthquakes occurred in the *i*-th bin

λ_i^j rate of earthquake occurrence for the *i*-th bin and *j*-th model.

$L_i^j = L(\omega_i | \lambda_i^j)$ log-likelihood calculated for the *i*-th bin and *j*-th model

90

91 The joint log-likelihood for the *j*-th model is calculated as

$$92 \quad L^j = \sum_{i=1}^n L(\omega_i | \lambda_i^j) \quad (1)$$

93 where *n* is the number of bins.

94 In order to get numbers from equation (1) $L(\omega_i | \lambda_i^j)$ must be defined. The basic assumption that
 95 stands behind the CSEP/RELM testing procedure is that earthquakes are assumed to occur in each
 96 bin according to a Poisson process with the rate specified by the model (Schorlemmer et al., 2007).

97 Note that this assumption is associated with the CSEP/RELM testing procedure not with the
 98 loglikelihood tests that can manage any kind of arbitrary distributions. Therefore, equation (1)
 99 becomes

$$L^j = \sum_{i=1}^n L(\omega_i | \lambda_i^j) = \sum_{i=1}^n (-\lambda_i^j + \omega_i \ln \lambda_i^j - \ln \omega_i!) \quad (2)$$

101 This assumption is crucial and a careful evaluation of its validity is mandatory to fully understand
 102 the CSEP/RELM tests. This assumption means that the bins are spatially and temporally
 103 independent, and the number of earthquakes in time has a variance equal to the average. Although
 104 some authors have already categorized such assumptions as "unlikely" and foresee possible
 105 inconsistencies of the tests (e.g., Werner and Sornette, 2008), the consequences have never been
 106 explored in detail. Moreover, we argue that the current use of this testing procedure in CSEP
 107 experiments may lead to think that the departures from this hypothesis could be considered as
 108 negligible.

109 The log-likelihood obtained by equation (2) is used to get the significance level of the tests through
 110 simulations. The L -test compares the observed log-likelihood value (see equation (2)) with a
 111 prefixed number of synthetic values obtained under the Poisson assumption for each bin, i.e.,
 112 simulating records where each bin has a number of earthquakes generated according to a Poisson
 113 process with the rate given by the model. The quantile score γ^j for the j -th model is the fraction of
 114 simulated likelihood values that are less or equal to the observed L . This quantile score can be
 115 considered the p-value of the test. Note that, compared to the analyses performed by Schorlemmer
 116 et al. (2007) and Werner and Sornette (2008), here we do not consider the inclusion of
 117 *uncertainties*, because we aim to explore the tests in an optimal situation, i.e., with negligible
 118 uncertainty in the observations.

119 Schorlemmer et al. (2007) discussed the case in which a model can pass the L -test even if it is
 120 wrong. For this reason, the authors proposed a second test, the N -test, that checks if the total
 121 number of forecasted events is compatible with the observed number. In this case the quantile score,

122 δ^j , is the probability to have no more than the observed number of events by a Poisson process
123 with a rate given by the model. In this case the test is two-sided, checking both possible over-
124 prediction and under-prediction. To summarize, a model is "good" (*reliable*) if it is not rejected by
125 both L and N tests. Only if the model passes these tests, then it is considered in the R -test, where it
126 is compared to other reliable models. In the next section, we explore the performances of the L - and
127 N -tests applied to synthetic catalogs. The goal is to check, in a controlled experiment, if the
128 proportion of rejections of the "right" model is comparable to the significance level of the test. We
129 anticipate that possible departures may point to inconsistencies of the Poisson variability for each
130 bin assumed in the CSEP/RELM testing procedure.

131

132 **3. Application of the CSEP/RELM testing procedure to synthetic catalogs.**

133 In order to evaluate quantitatively the performances of CSEP/RELM testing procedure, we use
134 these tests in a controlled experiment where we know exactly the model that generates earthquakes.
135 The experiment can be described in three steps:

136 1. We generate 100 synthetic catalogues that we call "pseudo-real catalogs". Specifically we
137 simulate two sets of 100 pseudo-real catalogs: one is consistent with a stationary non-homogeneous
138 Poisson process, and another that is consistent with the well-known Epidemic-Type Aftershocks
139 Sequence (ETAS; e.g., Ogata 1998) model. The generation of the ETAS pseudo-real catalogs is
140 described in Appendix A and mimics the 1992 Landers sequence.

141 2. We generate one-day forecasts for a period of 10 days after the mainshock using exactly the same
142 models and relative parameters that generate the pseudo-real catalogs. After each one-day forecast,
143 the history is updated to take into account all events that occurred before the starting time of the
144 next forecast. The forecasts are computed and evaluated in terms of expected number of events with
145 magnitude above M_1 3.0 in each cell C_i of a grid, with a spacing of $0.1^\circ \times 0.1^\circ$ and covering the target

146 region $[-117.5^\circ\text{W}/33.25^\circ\text{N} - -115.5^\circ\text{W}/35.5^\circ\text{N}]$. Specifically for each cell C_i and for each time
 147 window T_j we compute the relative forecast rate λ_i^j by the formula

$$148 \quad \lambda_i^j = \int_{T_j} \iint_{C_i} \int_{M_c}^{M_{\max}} \lambda(t, x, y, m | H_t) dt dx dy dm \quad (3)$$

149 where $\lambda(t, x, y | \mathcal{H}_t)$ is the space-time conditional intensity defined by Poisson and ETAS models (see
 150 Appendix A), M_c and M_{\max} are the minimum and maximum magnitude considered. The seismic
 151 history H_t , i.e. the information coming from the events that occurred before the time t , is crucial for
 152 time-dependent models, such as the ETAS model. On the other hand, the Poisson rate is
 153 independent of H_t and the time t . For the ETAS model we include in seismic history H_t the
 154 parameters of earthquakes that occurred before the time window T_j . To take into account the
 155 expected triggering effect of events that occurred during T_j , we simulate 1000 different stochastic
 156 realizations of the model inside the time window T_j and then we calculate for each bin the mean and
 157 the variance of predictions λ_i^j coming from each of these synthetic realizations.

158 3. We compare each one-day forecast with each pseudo-real catalog for both classes of models
 159 (Poisson and ETAS). For each of 100 pseudo-real catalogs we apply the N and L tests in order to
 160 verify the agreement between observations and forecasts. In this case, the model is certainly right;
 161 therefore we expect to see a number of rejections by both tests comparable to the significance level
 162 used.

163 In Figure 1 we show the fraction of rejections of both L (one tail test) and N -tests (two tails test) on
 164 100 ETAS pseudo-real catalogs at significance level 0.05, for daily and cumulative tests, and for
 165 each time window T_j . The plots show that the proportions of rejections of N -test are above 30% (see
 166 Figure 1a), much larger than the theoretical fraction (i.e., 5%). Similar results are found for the L -
 167 test (see Figure 1b), computed on whole region, for which the fraction of rejections is above 20%.

168 In order to verify the spatial distribution of L -test failures we show in Figure 2 the maps of quantile
 169 scores γ_j^i for each time window. The figure shows that the failures are mainly near Landers and Big
 170 Bear locations, where the number of events is larger and the spatial clustering is more evident.

171 The same analyses on Poissonian catalogues show that the fractions of rejections for both tests are
172 in perfect agreement with the significance level (0.05) adopted (see Figure 3).

173 To explain one of the possible reasons for this discrepancy, we report in Figure 4, the ratio between
174 mean and variance of the number of events recorded into 1000 synthetic ETAS catalogues,
175 simulated following the same rules used for the 100 pseudo-real catalogs (see Appendix A). This
176 ratio is much smaller than the unity, the value that characterizes the Poisson distribution (see Figure
177 4). This proves that the variability of the number of events is much larger than that expected in the
178 case of a Poisson process. By performing a Chi-squared test, the Poisson distribution is rejected for
179 all time-windows at a significance level of 0.01, and this independent of how the data are regrouped
180 to compare expected and observed distributions.

181 To quantify the differences between the variability of the seismic rate due to Poisson and ETAS
182 distributions, we plot in Figure 5 the differences of their 95% confidence bounds. Specifically, for
183 each pseudo-real ETAS catalog and for each day, we compute the variability of the seismic rate
184 $\Delta\alpha_{95\%}^{POISSON}$ expected by the Poisson distribution and assumed by CSEP tests; this value is compared
185 with the empirical variability $\Delta\alpha_{95\%}^{ETAS}$ of the ETAS distribution that has been calculated numerically
186 by the 1000 synthetic rates used for producing forecasts. Figure 5 shows the average of the
187 differences $\Delta\alpha_{95\%}^{ETAS} - \Delta\alpha_{95\%}^{POISSON}$ calculated for 100 pseudo-real catalogs. The positive differences
188 mean that the variability for the ETAS model is much larger than the variability of the Poisson
189 distribution. Interestingly, this difference decreases with time, implying that this difference becomes
190 less serious when the seismic rate tends to decrease.

191

192 **3. Discussion and conclusions.**

193 In this paper we show that part of the CSEP/RELM testing procedure does not perform correctly for
194 a widely used class of models, i.e., the ETAS models. Specifically, by reproducing the CSEP
195 experiment on “pseudo-real” ETAS catalogs – for which we know the right model – we find that

196 the rejections are much more than expected. We identify one main reason for this deficiency: the
197 assumption that the number of earthquakes per bin has a Poisson distribution does not hold for
198 ETAS models. The latter have a variability of occurrences much larger than what predicted by a
199 Poisson distribution. The underestimation of the variability made under the Poisson hypothesis
200 unavoidably leads to a high rejection frequency during the CSEP experiments, at least for the ETAS
201 class of models. It is worth noting that a higher variability compared to what assumed by the
202 Poisson hypothesis is also observed on real catalogs (e.g., Saichev and Sornette, 2007; Kagan, 2009
203 and references therein) possibly (but not necessarily) leading to a wide generalization of the
204 conclusions reported in this paper (see also Schorlemmer et al., 2010). These results may be
205 generalized in this way: forecasting models that produce a higher variability of the seismic rates
206 compared to the Poisson process may be rejected too often also when they represent an accurate
207 representation of the observed spatio-temporal evolution of the seismicity. On the other hand, we
208 also foresee that forecasting models producing a variability of the seismic rates smaller than that
209 expected in the case of a Poisson process may be not rejected often enough even in case they do not
210 represent an accurate representation of the seismicity. Figure 2 shows also another interesting
211 departure from the Poisson distribution. Rejected bins appear clustered in space. The Poisson
212 distribution assumes that the seismic variability per bin is conditioned only by the seismic rate of
213 the model. Actually, the observed rate in a bin is also conditioned by the seismicity occurred in the
214 adjacent bins during the forecasting time window; this component is neglected in the testing phase
215 and it may play an important role on the results of the L-test.

216 In this paper we have investigated a strongly clustered sequence (pseudo real catalogs mimicking an
217 aftershock sequence) that is characterized by bins with a large number of events. In other cases,
218 such as the one-day forecasts during a quiet period or the forecast of large events ($M \geq 5.0$) in a 5-
219 year time period, the expected number of events is probably much smaller. In these cases, the bias
220 may be less serious as showed by Figure 1 (cf. the rejection rates for $M3+$ and $M4+$ events) and

221 Figure 5, and also as expected by the theory of hypothesis testing (basically, the fewer the data, the
222 more difficult is to reject an hypothesis).

223 Although these results indicate a bias of the current testing procedures of the CSEP experiments, we
224 stress that these experiment remain of paramount importance and they are unavoidable if we wish to
225 maintain earthquake forecasting in a scientific domain that requires formulation of hypothesis and
226 testing. The lesson to be learned is that some of the CSEP/RELM testing procedures should be
227 improved and/or implemented. Specifically, in order to get reliable results, we argue that the
228 CSEP/RELM suite of tests needs a significant revision. We identify three possible strategies that
229 could be implemented for current and future experiments:

230 1. Each forecasting model has to provide the likelihood function. This allows the likelihood tests to
231 be applied correctly because the Poisson assumption of the seismic rate variability is no longer
232 necessary, and other goodness-of-fit tests and skill measures may be applied, like the residuals
233 analysis (Ogata 1998; Marzocchi and Lombardi, 2009) and the Information Gain (e.g., Daley and
234 Vere-Jones, 2003). Notably, this approach would also avoid potential biases in the testing phase due
235 to the spatial correlation of the rejected bins (see figure 2). This is maybe the optimal choice from a
236 statistical point of view, but it is not applicable to models that do not have a likelihood function,
237 such as many pattern recognition algorithms.

238 2. The forecasts have to be described by a distribution of the expected number of earthquakes (see
239 also Werner and Sornette 2008), not by a single value as now. For example, the forecasts may be
240 composed by 1000 expected number of events, from which a central value and the dispersion can be
241 easily retrieved (see Marzocchi and Lombardi, 2009). This strategy is in principle applicable to
242 every model, but it would require a change in the CSEP procedures. In our mind, this option is
243 probably the easiest to implement for future experiments, but it is inapplicable to the present
244 forecasts that are composed just by one single expected number of earthquakes. Moreover, being
245 still based on binning forecasts, we remark that this strategy would not avoid possible biases
246 induced by the spatial correlation of the bins; a careful analysis of such potential bias is required.

247 3. The model-based variability of the number of earthquakes in each bin may be set by some
248 empirical rules that take into account the higher variability that characterize many models. This is
249 widely applicable for all models and all experiments so far completed or running, but certainly it
250 raises important technical problems. The first one is the introduction of a key parameter (i.e. the
251 dispersion) *after* the forecasts have been made. This would corrupt the prospective philosophy of
252 the experiments. Second, the choice of the empirical adjustment rule becomes critical for the
253 evaluation process. Unavoidably, this choice would raise a lot of debate about what is the best
254 adjustment rule, and if different rules should be applied to different models. In any case, it may be
255 difficult to establish these rules objectively and independently from the modelers.

256

257 **Data and Resources**

258 The Landers earthquake data were obtained from Southern California Earthquake Data Center,
259 website (<http://data.scec.org/research/altcatalogs.html>). The maps were made using the Generic
260 Mapping Tools (www.soest.hawaii.edu/gmt). The MATLAB GNU codes used in the present work
261 to run the N and L tests have been provided by the Southern California Earthquake Center CSEP
262 software development team.

263

264 **Acknowledgments**

265 The researches that motivated this study have been promoted in the framework of EC project
266 Network of Research Infrastructures for European Seismology, NERIES, www.neries-eu.org. A.M.
267 Lombardi has been supported by the EC project NERIES contract 026130. We thank Jeremy Zechar
268 and Max Werner for useful discussions. We thank Jochen Woessner for advising on the CSEP tests.

269

270 **References**

271 Daley D.J. and D. Vere-Jones (2003), *An Introduction to the Theory of Point Processes*, Springer-
272 Verlag, New York, 2-nd ed., Vol. 1, pp. 469.

273 ICEF (International Commission on Earthquake Forecasting for Civil Protection) (2009).
274 Operational Earthquake Forecasting: State of Knowledge and Guidelines for Utilization.
275 Report for Italian Civil Protection .

276 Jordan, T.H. (2006). Earthquake Predictability: Brick by brick, *Seismol.Res.Lett.*, 77(1), 3-6.

277 Kagan Y.Y. (2009). Statistical distributions of earthquake numbers: consequence of branching
278 process, *Geophys. J. Int.*, submitted.

279 Kagan Y.Y., D.D. Jackson (1994). Long-term probabilistic forecasting of earthquakes, *J. Geophys.*
280 *Res.*, 99, 13685-13700.

281 Kagan Y. Y., D. D. Jackson (1995). New seismic gap hypothesis: Five years after. *J. Geophys. Res.*,
282 100, 3943-3959.

283 Marzocchi W., L. Sandri, E. Boschi (2003). On the validation of earthquake-forecasting models: the
284 case of pattern recognition algorithms. *Bull. Seismol. Soc. Am.*, 93, 1994-2004.

285 Marzocchi W., A.M. Lombardi (2009). Real-time forecasting following a damaging earthquake.
286 *Geophys. Res. Lett.*, 36, L21302, doi:10.1029/2009GL040233.

287 Ogata, Y. (1998). Space-Time Point-Process Models for Earthquake Occurrences, *Ann. Inst. Statist.*
288 *Math.* 50(2), 379-402.

289 Saichev A., D. Sornette (2007). Power law distribution of seismic rates, *Tectonophysics*, 431, 7-13

290 Schorlemmer, D., and M. C. Gerstenberger (2007). RELM testing center. *Seismol.Res.Lett.*, 78(1),
291 30-36.

292 Schorlemmer, D., M.C. Gerstenberger, S. Wiemer, D.D. Jackson and D.A. Rhoades (2007).
293 Earthquake Likelihood Model Testing, *Seismol.Res.Lett.*, 78(1), 17-29.

294 Schorlemmer D., J.D. Zechar, M.J. Werner, E.H. Field, D.D. Jackson, T.H. Jordan (2010). First
295 results of the Regional Earthquake Likelihood Models experiment, *Pure Applied Geophys.*,
296 in press.

297 Werner M. J., and D. Sornette (2008), Magnitude uncertainties impact seismic rate estimates,
298 forecasts, and predictability experiments, *J. Geophys. Res.* 113, B08302,
299 doi:10.1029/2007JB005427.

300 Zechar J.D., T.H. Jordan (2008), Testing alarm-based earthquake predictions, *Geophys. J. Int.*, 172,
301 715-724.

302 Zechar J.D., D. Schorlemmer, M. Liukis, J. Yu, F. Euchner, P.J. Macheling, and T.H. Jordan
303 (2009), The Collaboratory for the Study of Earthquake Predictability perspective on
304 computational earthquake science, *Concurrency and Computation: Practice and Experience*,
305 doi: 10.1002/cpe.1519

306

307

308

309

310

311

312

313

314

315

316

317

318

319

320

321

322

323 **Figure Captions**

324

325 **Figure 1:** Fractions of rejections of the daily L and N -test on 100 pseudo-real ETAS catalogs.

326 **Figure 2:** Spatial distribution of fractions of rejections on 100 pseudo-real ETAS catalogs for L -test
327 conducted on 10 time windows.

328 **Figure 3:** The same of Figure 1 but for pseudo-real Poisson catalogs.

329 **Figure 4:** Ratio between mean and variance of events recorded in 1000 ETAS pseudo-real catalogs
330 for 10 time windows.

331 **Figure 5:** Difference between the 95% confidence intervals of the ETAS and Poisson distributions
332 as a function of the forecasting time window; each point represents the average of the differences
333 calculated for the 100 ETAS pseudo-real catalogs used for L and N -tests.

334

335

336

337

338

339

340

341

342

343

344

345

346

347

348

349 **APPENDIX A. Generating the pseudo-real synthetic catalogs**

350 In this appendix, we report the strategy adopted to generate ETAS and Poissonian pseudo-real
351 catalogs.

352 The total space-time conditional intensity $\lambda(t,x,y/\mathcal{H}_t)$ of the ETAS model (i.e. the probability of an
353 earthquake occurring in the infinitesimal space-time volume conditioned to all past history) is
354 defined by equation:

355

$$356 \quad \lambda(t,x,y,m/\mathcal{H}_t) = \left[vu(x,y) + \sum_{t_i < t} \frac{K}{(t-t_i+c)^p} e^{\alpha(M_i-M_c)} \frac{c_{d,q,\gamma}^i}{\left[r_i^2 + \left(de^{\gamma(M_i-M_c)} \right)^2 \right]^q} \right] \beta e^{\beta(m-M_c)} \quad (A1)$$

357

358 where $\mathcal{H}_t = \{(t_i, x_i, y_i, M_i); t_i < t\}$ is the observation history up time t , M_c is the completeness
359 magnitude of the catalog, $u(x,y)$ is the spatial probability density function (PDF) of background
360 events, $c_{d,q,\gamma}^i = \frac{q-1}{\pi} [(de^{\gamma(M_i-M_c)})^2]^{q-1}$ is the normalization constant of the spatial PDF for
361 triggered events, and r_i is the distance between location (x,y) and the epicenter of i -th event (x_i, y_i)
362 (Lombardi et al., 2009). Finally $\beta = b \cdot \ln(10)$ is the parameter of the well-known Gutenberg-Richter
363 Law (Gutenberg and Richter, 1954), assumed as distribution for magnitude of all events.

364 The set of parameters $\Theta = (v, K, c, p, \alpha, d, q, \gamma, \beta)$ of the model, for the events occurred within a
365 time interval $[T_1, T_2]$ and a region R , can be estimated by maximizing the log-likelihood function
366 (Daley and Vere-Jones, 2003), given by

$$367 \quad \log L(\Theta) = \sum_{i=1}^N \log \lambda(t_i, x_i, y_i, m_i / H_{t_i}) - \int_{T_1}^{T_2} \int_R \int_{M_c}^{M_{max}} \lambda(t, x, y, m / H_t) dt dx dy dm \quad (A2)$$

368 A careful method to obtain the best parameters of the model is the iteration algorithm developed by
369 Zhuang et al. (2002), providing also an estimation of the PDF $u(x,y)$ for background events.

370 Our pseudo-real ETAS catalogs are simulated in agreement with the ETAS model estimated for the
371 region hit by the Landers earthquake. Specifically we use the relocated data set (Hauksson and
372 Shearer, 2005) recorded by the California Institute of Technology/U.S. Geological Survey (CIT /
373 USGS) Southern California Seismic Network and available at the SCEDC (Southern California
374 Earthquake Data Center) website (<http://data.scec.org/research/altcatalogs.html>). We consider
375 earthquakes with a depth less than 30 km and a magnitude above 3.0, occurred from Jan 1 1984 to
376 Dec 31 2004 and located in the region $[-119.0^\circ\text{W}/32.5^\circ\text{N} - -115.0^\circ\text{W}/36.5^\circ\text{N}]$ (5757 events). The
377 parameters estimated by using the procedure proposed by Zhuang et al. (2002) are listed in Table

378 A1. We perform simulations by including in the past history the real observed seismicity above
 379 magnitude 3.0, occurred before July 1 1992, 3 days after the $M_L 7.3$ Landers mainshock. In this way
 380 we take into account knowledge coming from the initial phase of the sequence, including also the
 381 $M_L 6.4$ Big Bear aftershock.

382 We simulate the Poisson pseudo-real catalogs by imposing a rate of 60 day^{-1} and adopting the PDF
 383 $u(x,y)$, estimated for the ETAS model, for the spatial distribution of events. All pseudo-real catalogs
 384 recover a time period of 10 days. We remark that we intend to perform simulations by reproducing
 385 the type of forecasts usually tested in CSEP laboratories, no matter the specific region or time
 386 period we consider.

387 In order to verify the reliability of our pseudo-real catalogs, we analyze their residuals. The residual
 388 analysis is a common diagnostic technique for stochastic point processes based on transformation of
 389 the time axis t into a new scale τ by the increasing function

$$390 \quad \tau = \Lambda(t) = \int_{T_{start}}^t dt \int_R dx dy \int_{M_c}^{M_{max}} dm \lambda(t,x,y,m/\mathcal{H}_t) \quad (A3)$$

391 where T_{start} is the starting time of the observation history H_t (Ogata, 1998). The random variable τ
 392 represents the expected number of occurrences in time period $[T_{start}, t]$. If a model with conditional
 393 intensity $\lambda(t,x,y,m/\mathcal{H}_t)$ describes the temporal evolution of the process, the transformed data τ_i
 394 $=\Lambda(t_i)$, known in statistical seismology with the name of *residuals*, are expected to behave like a
 395 stationary Poisson process with the unit rate (Ogata, 1998); i.e. the values $\Delta\tau_i = \tau_{i+1} - \tau_i$ are
 396 independent and exponentially distributed (with mean equal to 1) random variables. We check this
 397 hypothesis for residuals by means of two nonparametric tests: the Runs test, to verify the reliability
 398 of the independence property, and the one-sample Kolmogorov-Smirnov (KS1) test, to check the
 399 standard exponential distribution (Gibbons and Chakraborti, 2003; Lombardi and Marzocchi, 2007).
 400 Specifically the Runs-test can be used to test if a process is not auto-correlated and consists in
 401 testing the randomness of runs, i.e. of uninterrupted subsequences of values above or below the
 402 mean (see Gibbons and Chakraborti, 2003; Lombardi and Marzocchi, 2007 for details). We use
 403 both tests because all goodness-of-fit tests (as KS1) are ineffective to check the presence of a
 404 memory in the time series. Hence, any discrepancy of residuals by Poisson hypothesis, identified by
 405 just one or both tests, is a sign of inadequacy of ETAS model to explain all basic features of
 406 analyzed seismicity. We stress that this check analysis is similar to the RELM/CSEP N -test. As the
 407 N -test, it consists in a comparison between the observed and the expected total number of events
 408 and it is directed to highlight under or over-prediction. On the other side the residual analysis does
 409 not need the discretization of the temporal scale in time bins. As explained along the text, this is a
 410 crucial point of RELM/CSEP tests. In Figure A1 we show the empirical cumulative function of p-

411 values of KS1 and Runs tests, for the 100 pseudo-real ETAS catalogs, together with the 99%
412 confidence bounds. The confidence level is calculated assuming that for each point of the curve the
413 expected fraction of rejection is given by the p-value reported on the x-axis, and the variability (1
414 sigma) is given by $\sqrt{p(1-p)/N}$. Note that, for both tests the cumulative distribution is inside the
415 99% confidence interval.

416

417 **References**

- 418 Daley, D.J. and D. Vere-Jones (2003). *An Introduction to the Theory of Point Processes*, Springer-
419 Verlag, New York, 2-nd ed., Vol. 1, pp. 469.
- 420 Gibbons, J.D. and S. Chakraborti (2003). *Non-parametric Statistical Inference*, 4th ed., rev. and
421 expanded, New York: Marcel Dekker, 645 pp.
- 422 Gutenberg, B. and C.F. Richter (1954). *Seismicity of the Earth and Associated Phenomena*,
423 Princeton, pp. 273.
- 424 Hauksson, E. and P. Shearer (2005). Southern California Hypocenter Relocation with Waveform
425 Cross-Correlation, Part 1: Results Using the Double-Difference Method, *Bull. Seismol. Soc.*
426 *Am.*, **95** (3), 896–903, doi:10.1785/0120040167.
- 427 Lombardi, A. M., and W. Marzocchi (2007). Evidence of clustering and nonstationarity in the time
428 distribution of large worldwide earthquakes, *J. Geophys. Res.*, **112**, B02303,
429 doi:10.1029/2006JB004568.
- 430 Lombardi, A.M., M. Cocco and W. Marzocchi (2009). On the increase of background seismicity
431 rate during the 1997-1998 Umbria-Marche (central Italy) sequence: apparent variation or
432 fluid-driven triggering? Submitted to *Bull. Seismol. Soc. Am.*
- 433 Ogata, Y. (1998). Space-Time Point-Process Models for Earthquake Occurrences, *Ann. Inst. Statist.*
434 *Math.* **50**(2), 379-402.
- 435 Zhuang, J., Y. Ogata and D. Vere-Jones (2002). Stochastic declustering of space-time earthquake
436 occurrence, *J. Am. Stat. Assoc.*, **97**, 369-380.

437

438

438 **Figure Captions**

439 **Figure A1:** Cumulative function of the empirical p-values (solid black lines) for KS1 (panel a) and
440 RUNS (panel b) Test applied to Residuals of 100 simulated ETAS catalogues. Dashed gray lines
441 mark the 99% confidence bounds.

442
443
444
445
446
447
448
449
450
451
452
453
454
455
456
457
458
459
460
461
462
463
464
465
466
467
468
469
470
471

| Parameter | Value |
|----------------|---|
| ν | 0.10 ± 0.004 (day ⁻¹) |
| K | 0.043 ± 0.002 (day ^{p-1}) |
| p | 1.20 ± 0.01 |
| c | 0.030 ± 0.004 (day) |
| α | 1.20 ± 0.03 (mag ⁻¹) |
| d | 0.30 ± 0.01 (km) |
| q | $\equiv 1.5$ |
| γ | 0.60 ± 0.03 (mag ⁻¹) |
| Log-likelihood | -21277.5 |

472

473 **TableA1:** Maximum Likelihood parameters (with relative errors) and log-likelihood of ETAS
474 model for Landers region seismicity [-119.0° W/32.5° N – -115.0° W/36.5° N]
475 ($M_c = 3.0$; Jan 1 1984 – Dec 31 2004; 5757 events)

476

477

478

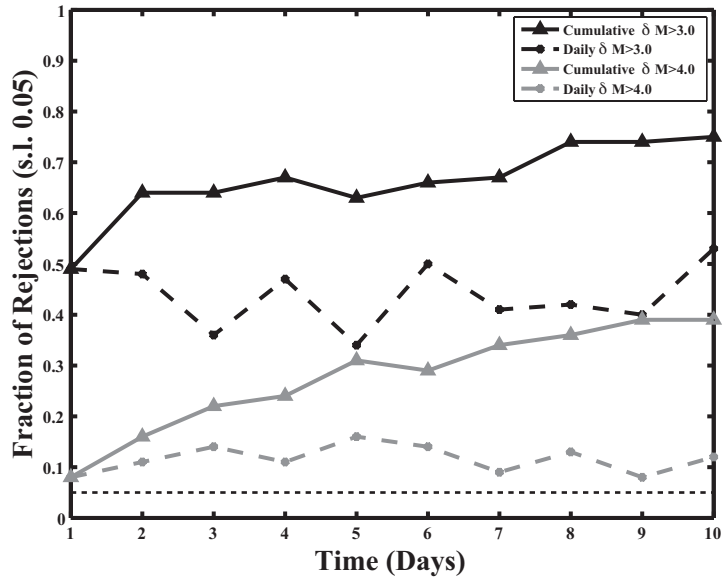
479

480

481

482

N-test



L-test

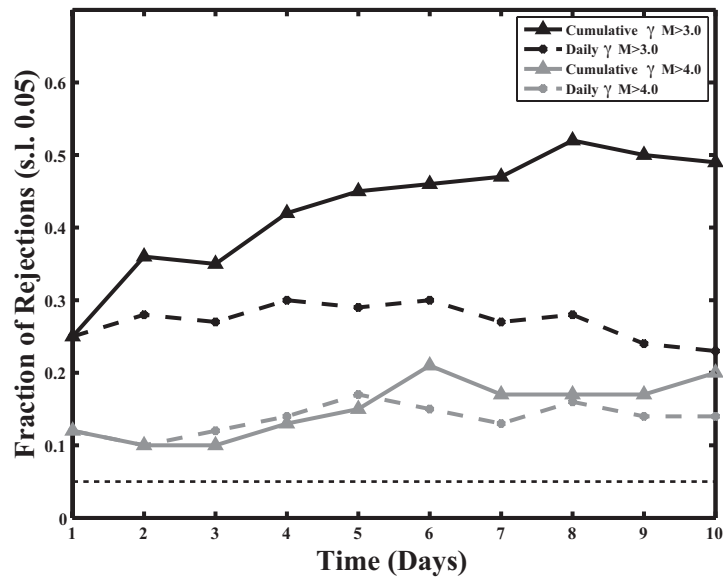


Figure 1

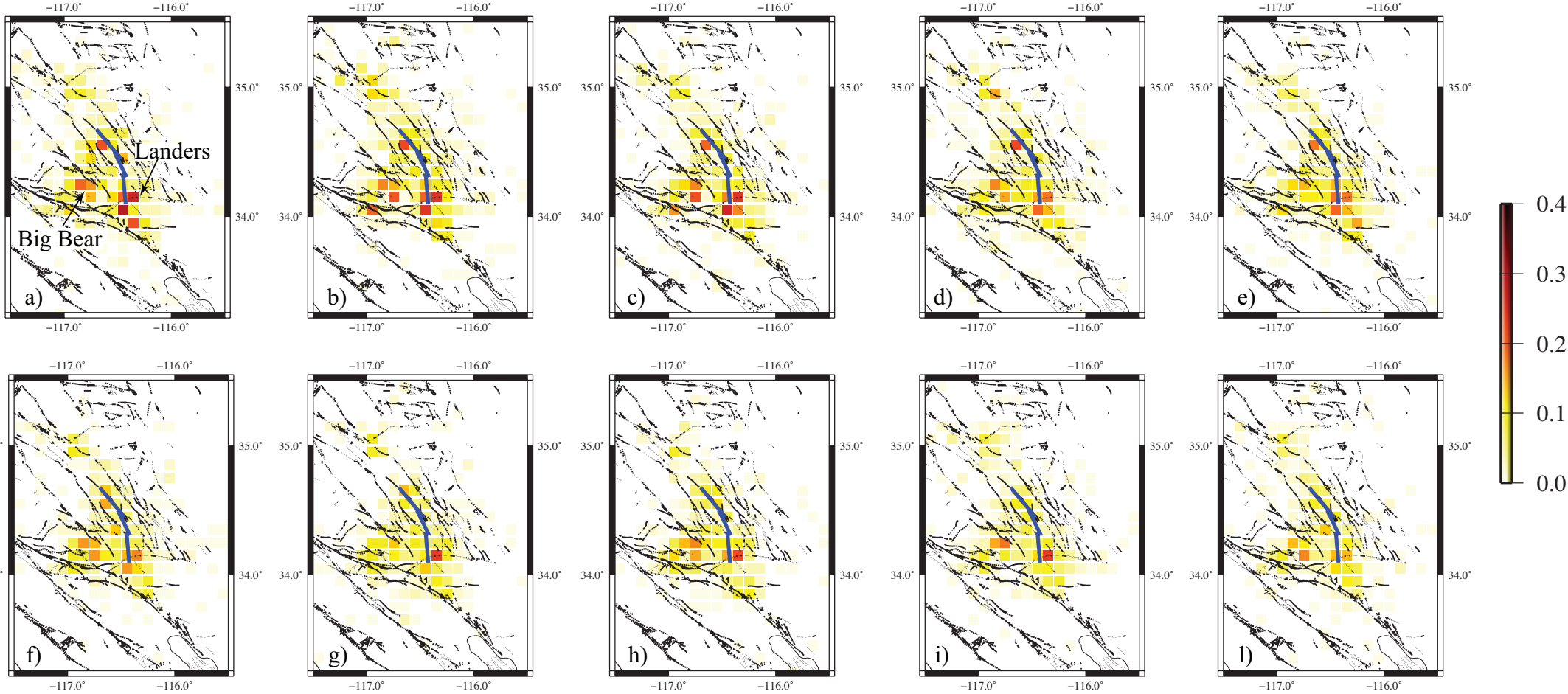


Figure 2

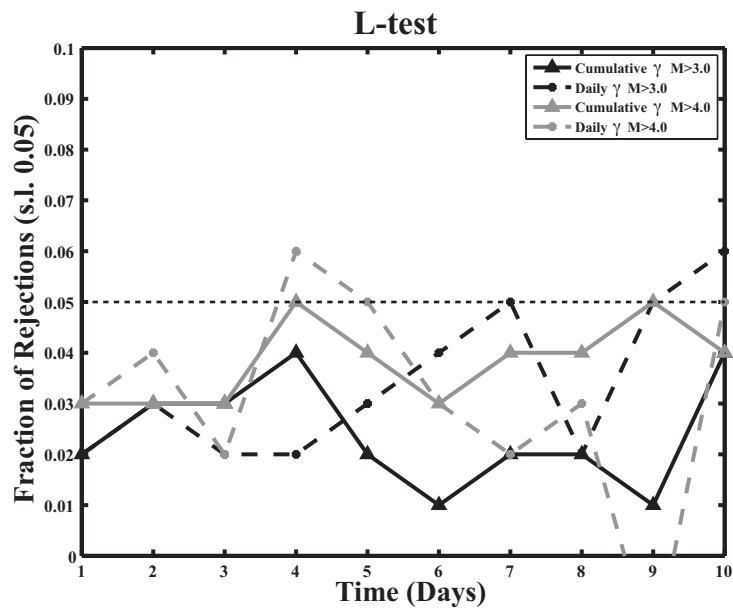
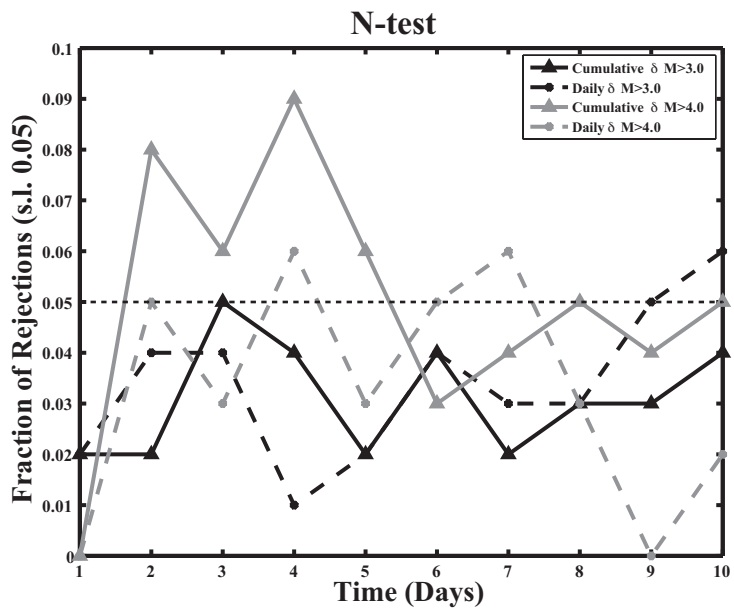


Figure 3

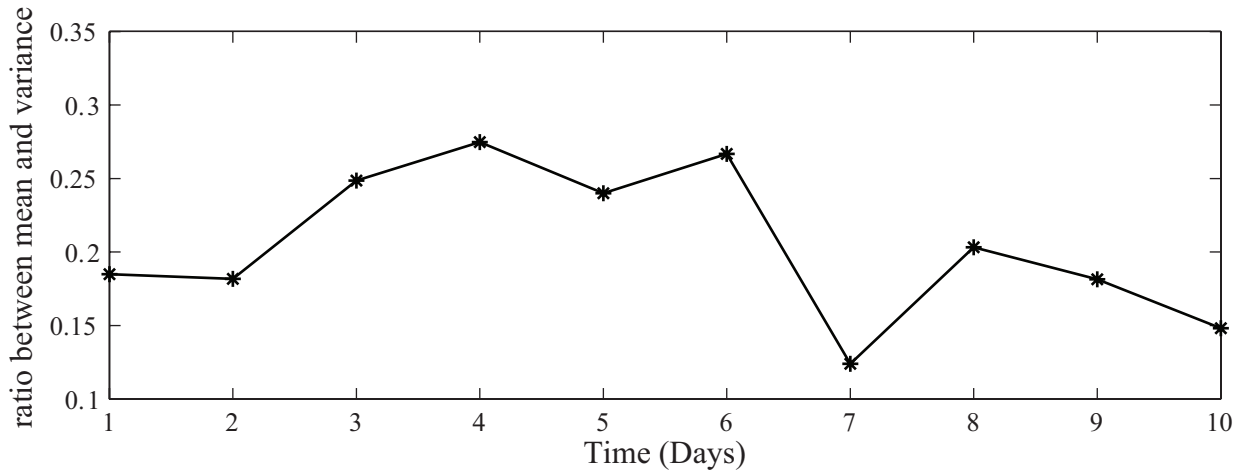
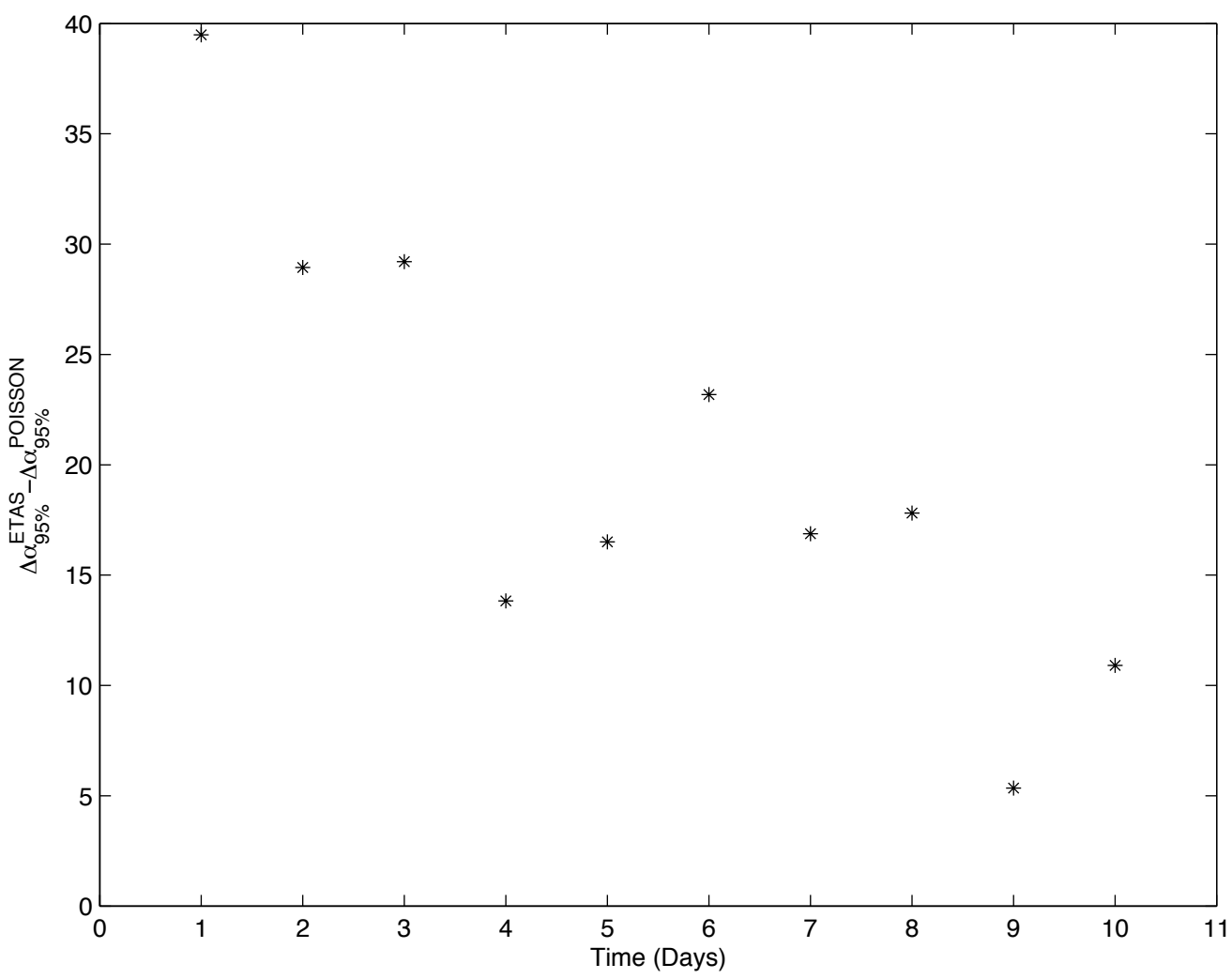


Figure 4



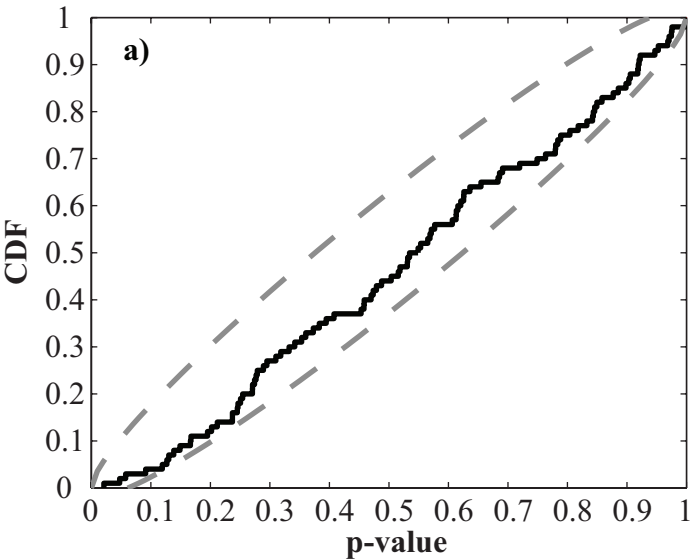
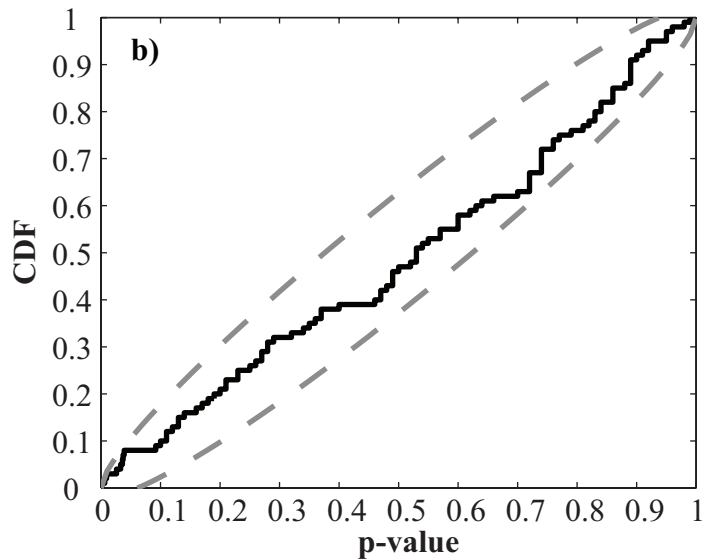
KS1 TEST**RUNS TEST**

Figure A1